Electrochemical Separation of Alkaline-Earth Elements from Molten Salts

Using Liquid Metal Electrodes

Thomas P. Nigl¹, Timothy Lichtenstein^{1,a}, Yuran Kong¹, Hojong Kim^{1*}

¹Materials Science and Engineering, The Pennsylvania State University,

University Park, PA 16802, United States

Author Addresses:

Thomas P. Nigl 231 Steidle Building University Park, PA 16802 tpn6@psu.edu

Timothy Lichtenstein 231 Steidle Building University Park, PA 16802 tvl5297@psu.edu

Yuran Kong 231 Steidle Building University Park, PA 16802 yxk42@psu.edu

Hojong Kim 406 Steidle Building University Park, PA 16802 huk29@psu.edu

Corresponding Author:

*E-mail: huk29@psu.edu. Tel: 814-865-3117. Fax: 814-865-2917

Abstract:

Closing the nuclear fuel cycle requires recycling used nuclear fuel. Additional waste is generated during recycling due to fission products accumulating in processing salts (LiCl-KCl). Reducing waste generated during recycling entails recovering alkaline-earth fission products (Ba²⁺/Sr²⁺) from molten chlorides with a minimal loss of bulk electrolyte constituents (Li⁺/K⁺). Electrochemical co-deposition of Ba²⁺/Li⁺ and Sr²⁺/Li⁺ into liquid metal (Bi, Sb, Sn, Pb) and alloy (Bi-Sb) electrodes was investigated in LiCl-KCl-(BaCl₂, SrCl₂) electrolytes at 500 °C and 650 °C. For the pure Bi (500 °C) and Sb (650 °C) electrodes, the greatest percentage of charge was used to deposit Ba and Sr. Effective recovery of Ba/Sr by liquid Bi and Sb electrodes is supported via experimentally determined activity values of Ba/Sr in Bi and Sb. Alloying Sb with Bi increased Ba recovery but decreased Sr recovery, as compared to recovery using the liquid Bi electrode. The results suggest that alkaline-earth fission products can be recovered from molten chlorides by liquid metal electrodes via electrochemical separation, thereby providing a methodology to reduce the generation of nuclear waste from nuclear fuel recycling.

KEYWORDS:

Molten salts, Liquid metal electrodes, Electrochemical separations, Used nuclear fuel recycling, Nuclear fuel cycle, Electrorefining, Alkaline-earth metals

INTRODUCTION

Sustainable production of low-carbon nuclear energy requires closing the nuclear fuel cycle by recycling used nuclear fuel, for example, through pyroprocessing in molten salts. The essential step in pyroprocessing is electrorefining, in which uranium oxidizes out of the used fuel anode into a eutectic LiCl-KCl molten salt electrolyte at 500 °C and deposits at the cathode for recycling.¹ While uranium is separated from the used fuel, fission products (e.g. Sr, Ba) more electrochemically active than uranium oxidize into the electrolyte but accumulate as stable dissolved ions. The accumulation of fission products not only imparts decay heat to the system, but also changes the liquidus temperature of the electrolyte, complicating thermal management of the electrorefining process.^{2,3,4} Consequently, a portion of the processing salt (LiCl-KCl) is removed and disposed of, thereby increasing the volume of nuclear waste that can lead to health and environmental risks if not securely contained.⁵ To reduce nuclear waste from pyroprocessing, fission products must be separated with minimal removal of the processing salt. Of the fission products, the separation of alkaline-earth elements is particularly challenging since alkaline-earth salts (BaCl₂ and SrCl₂) are thermodynamically more stable than the processing salt. 6 In order to recover alkaline-earths from molten salts, this work studied strongly-interacting liquid metal electrodes (Sb, Bi, Sn, Pb) into which alkaline-earth fission products (Ba and Sr) can be electrodeposited in the liquid state.

Matsumiya et al. investigated liquid Pb, Sn, and Bi metals to recover Ba and Sr from NaCl-KCl-BaCl₂ at 727 °C and from NaCl-KCl-SrCl₂ at 800 °C, respectively.^{7,8} Based on the analysis of electrolysis products, they reported that the alkaline-earth (Ba or Sr) fission products were recovered by the liquid Pb and Sn electrodes, but not by the liquid Bi electrode (e.g., < 0.1 ppm for Sr); and postulated that an enhanced recovery capability of Pb and Sn, compared to Bi, originates from an extremely low activity coefficient (γ) of alkaline-earth metals in the liquid

metals, for example, $\gamma_{Ba(in\ Pb)}=1.5\times 10^{-9}$, $\gamma_{Ba(in\ Sn)}=1.5\times 10^{-10}$, and $\gamma_{Ba(in\ Bi)}=1.6\times 10^{-6}$ at 727 °C. In contrast, Lichtenstein et al. investigated the constant-current electrolysis of liquid Bi electrodes in ternary LiCl-KCl-SrCl₂/BaCl₂ (56.7-38.3-5 mol%) electrolytes at 500 °C, and reported substantial recovery of Ba (12 mol%) and Sr (6.5 mol%) in liquid Bi.⁹ They also postulated that the unique capability of liquid Bi for alkaline-earth recovery is attributed to the extremely low γ of alkaline-earth metals in liquid Bi, for example, $\gamma_{Ba}=1.6\times 10^{-15}$ and $\gamma_{Sr}=2.1\times 10^{-13}$ at 500 °C, as determined from emf measurements.^{10,11}

The comparison of results from Matsumiya et al. and Lichtenstein et al. clearly illustrates inconsistencies in the assessment of liquid Bi for alkaline-earth recovery as well as in the $\gamma_{\rm Ba}$ by nine orders of magnitude, inviting scrutiny into the capability of liquid metals for alkaline-earth recovery from molten salts. Thermodynamic properties of eight binary (Ba, Sr)-(Bi, Sb, Sn, Pb) alloys were investigated via emf measurements ($\Delta \overline{G} = -2FE = RT \ln a$) using solid CaF₂-BaF₂/SrF₂ electrolyte, shown in Fig. 1 for selected Ba/Sr mole fractions ($x_{\rm Ba/Sr} = 0.03$ -0.07). ^{10,11,12,13,14,15,16,17} A large emf value in these liquid metals (i.e., low γ) indicates strong chemical interactions between alkaline-earth and liquid metals; the degree of interactions is strongest for Sb, followed by Bi, Sn, and Pb for both Ba and Sr.

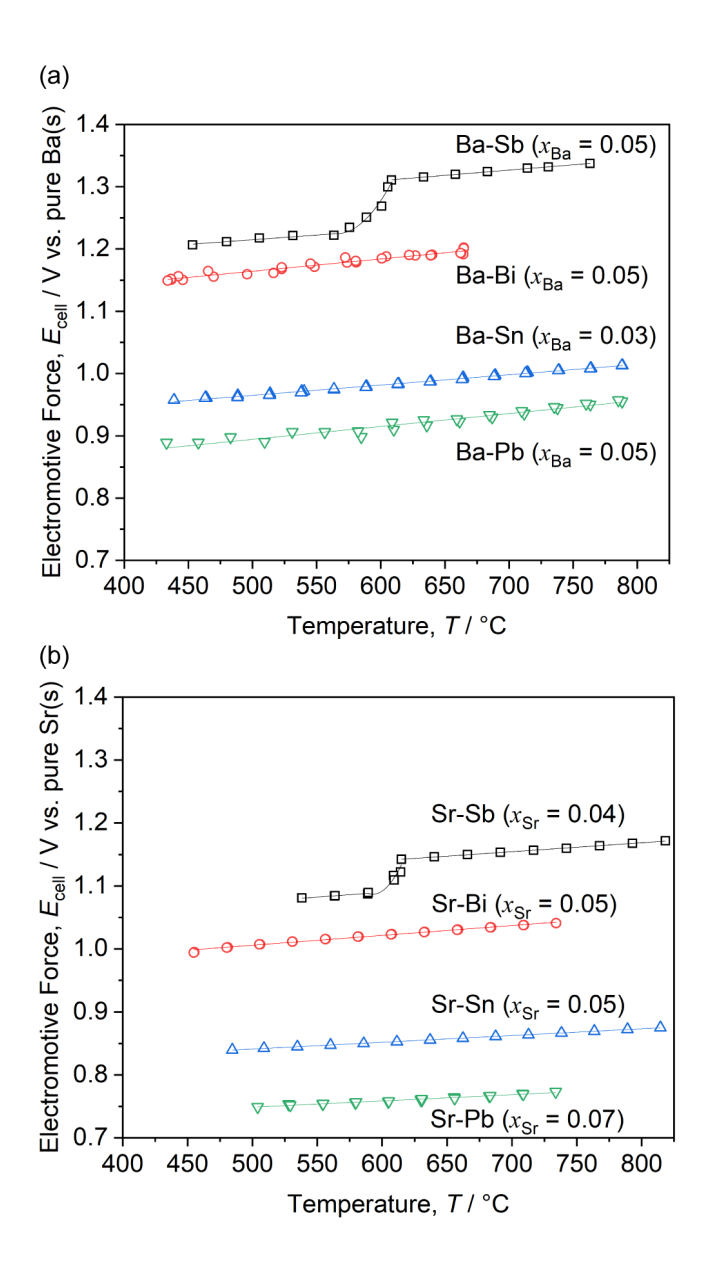


Figure 1: Emf as a function of temperature of (a) binary Ba-(Sb, Bi, Sn, Pb) alloys and (b) binary Sr-(Sb, Bi, Sn, Pb) alloys at selected mole fractions, where solid lines represent linear or curved fits. ^{10,11,12,13,14,15,16,17}

By leveraging the low γ of Ba and Sr in the liquid metals (Sb, Bi, Sn, and Pb), it is possible that liquid metal electrodes could be used to recover Ba and Sr and enable reuse of the processing salt. To evaluate the efficacy of liquid metal electrodes in separating Ba and Sr from molten salts, liquid metals (Bi, Sb, Sn, and Pb) were subjected to constant-current (-50 mA cm⁻²) electrolysis at 200 C g⁻¹ in ternary LiCl-KCl-BaCl₂/SrCl₂ electrolytes at 500 °C, with the exception of Sb at 650

 $^{\circ}$ C due to its high melting temperature ($T_{\rm m, Sb} = 631 \, ^{\circ}$ C). Three liquid Bi-Sb alloys (50-50, 60-40, 70-30 mol%) were also evaluated at 500 $^{\circ}$ C, utilizing the strong interactions of Sb and Bi with alkaline-earths at a lower temperature.

EXPERIMENTAL

Electrochemical cell components and assembly

All electrochemical cell components were prepared and assembled in an argon filled glovebox (< 0.5 ppm O_2 and H_2O) to prevent the hygroscopic electrolytes and reactive electrode materials from reacting with moisture and oxygen.

Electrolytes and Electrodes: Ternary LiCl-KCl-BaCl₂ and LiCl-KCl-SrCl₂ (56.7-38.3-5.0 mol%) electrolytes were prepared from appropriate weights of pure anhydrous salts: LiCl (99.9%, Alfa Aesar), KCl (99.95%, Alfa Aesar), SrCl₂ (99.5%, Alfa Aesar) and BaCl₂ (99.998%, Alfa Aesar) by vacuum-drying and premelting at 700 °C under Ar flow. Pure liquid metal electrodes were prepared by weighing 2.7 g of pure Bi (99.999%, Sigma Aldrich), Sb (99.999%, Alfa Aesar), Sn (99.9999+%, Alfa Aesar), or Pb (99.9%, Sigma Aldrich) pieces. Three Bi-Sb electrodes (50-50, 60-40, and 70-30 mol%) were prepared by weighing a total 2.7 g of Bi and Sb pieces. The liquid metal working electrodes (WE) were melted in a boron nitride (BN) crucible (Saint-Gobain Advanced Ceramics, Product No. AX05), using an induction heater (IH15A-2T, Across International) custom installed inside a glove box. The dimensions of the BN crucible were 15 mm in height, 12 mm outer diameter, 8 mm inner diameter, and 15 mm in depth, resulting in a nominal electrode surface area of 0.5 cm². As the metal pieces melted during induction heating, a tungsten wire (99.95%, Thermo Shield, 1 mm diameter) was inserted into the liquid metal to establish electrical contact.

A graphite cylinder (0.95 cm diameter, 3 cm length) was used as the counter electrode (CE) in the three-electrode cells. The cylinder was female-threaded at the top and electrically connected

to a male-threaded stainless-steel rod. The Ag/Ag⁺ reference electrode (RE) was constructed of a closed end mullite tube (6.4 mm in outer diameter and 45.7 cm in length) filled with 0.5 g of LiCl-KCl-1 wt.% AgCl electrolyte and a Ag wire (1 mm in diameter and 48.3 cm in length; 99.9%, Alfa Aesar). The LiCl-KCl-AgCl electrolyte was prepared by adding 1 wt.% AgCl (anhydrous, 99.998%, Sigma Aldrich) to eutectic LiCl-KCl and premelting the mixture using a similar procedure to prepare the bulk electrolytes.

Cell assembly: The electrodes and thermocouple were arranged inside an alumina crucible (60 mm in diameter and 100 mm in height; AdValue Technology). The tungsten wires and thermocouple were inserted through the stainless-steel flange, electrically insulated by mullite tubes, and sealed at the top of the mullite tubes with epoxy. About 70 g of the electrolyte was poured into the crucible over the electrodes. The assembled cell was then loaded into the stainless-steel vacuum chamber. The chamber was removed from the glove box and loaded into a crucible furnace. The cell was initially heated and vacuum-dried in the chamber using a similar procedure for preparing the electrolytes, and then heated to 650 °C for the Sb electrode or 500 °C for other low-melting electrodes, and held at temperature for 12 h to equilibrate the electrodes before measurements. The cell temperature was monitored and recorded using a data acquisition board (National Instruments, NI 9211).

Electrochemical measurements and characterization of electrolysis products

Constant-current electrolysis was conducted in a three-electrode cell. Each liquid metal WE was subjected to a constant cathodic current density ($j = -50 \text{ mA cm}^{-2}$) up to a specific charge of 200 C g⁻¹ using a potentiostat-galvanostat (Autolab PGSTAT302 N). After each electrolysis, the cell was cooled to room temperature and the electrode was isolated from the system. The electrode was then separated from the BN and rinsed with deionized water to remove entrained salt from the electrode surface. The electrode was divided into two parts: (1) for metallographic

characterization using a scanning electron microscope (SEM, FEI Quanta 200) fitted with energy dispersive X-ray spectroscopy (EDS), and (2) for chemical analysis using inductively coupled plasma-atomic emission spectroscopy (ICP-AES, Perkin-Elmer Optima 5300DV) with an accuracy of 4% of the measured value. The metallographic sample was mounted in epoxy and drypolished using a silicon carbide emery paper (up to 1200 grit). The remaining part of the electrode was pulverized into a fine powder with a mortar and pestle in a glovebox for chemical analysis by ICP-AES.

RESULTS AND DISCUSSION

Electrolysis and characterization of pure liquid metal electrodes

During constant-current electrolysis at j = -50 mA cm⁻², the potential of each electrode monotonically decreased (Figs. 2, 3). The potential of the Sb electrode was the most positive, followed by that of Bi, Sn, and Pb electrodes in both electrolytes, in accordance with the order of the emf results in Fig. 1.

According to the chemical analysis by SEM-EDS, Ba- or Sr-rich phases were observed in the nearly pure metal matrix of each liquid metal, confirming the reduction of Ba and Sr into the liquid metal electrodes (Figs. 2, 3). Upon solidification, electropositive Ba and Sr formed intermetallic compounds in each liquid metal that can be found in their respective binary phase diagrams, for example, the Ba-Sb (25-75 mol%) phase as BaSb₃ and the Sr-Bi (22-78 mol%) as SrBi₃. However, the composition of the Ba-Bi phase (38-62 mol%) was substantially different from the expected BaBi₃ compound, indicating the formation of a ternary Ba-Li-Bi compound and the co-deposition of Li. Recently, Ojwang and Bobev identified a new ternary Ba₇Li₁₁Bi₁₀ compound which has a Ba:Bi molar ratio of 41:59, similar to the ratio of 38:62 noted in this work by SEM-EDS.¹⁸

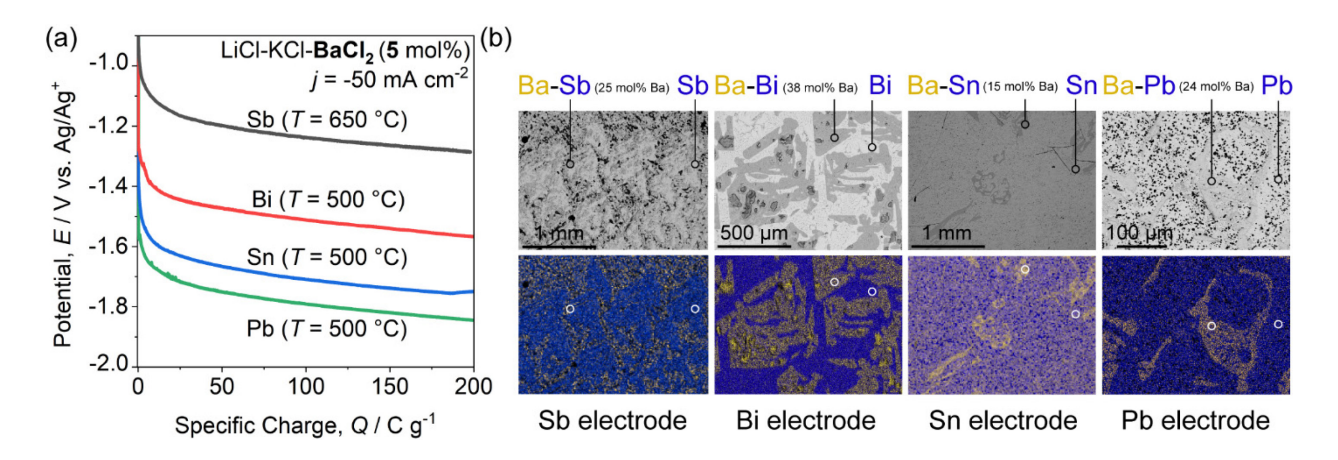


Figure 2: (a) Electrode potential of liquid metal electrodes (Sb, Bi, Sn, Pb) during electrolysis at j = -50 mA cm⁻² in LiCl-KCl-BaCl₂ electrolyte and (b) SEM and elemental X-ray mapping images after electrolysis at 500 °C or 650 °C for Sb (Ba = yellow, liquid metal = dark blue).

The co-deposition of Li also was also indicated from unidentified regions in SEM-EDS images beyond the instrument capability. For example, both Sr and Bi are depleted in a distinct dark region in the Sr-Bi image (Fig. 3) due to the presence of light-element Li, which is confirmed via ICP-AES analysis in the following section.

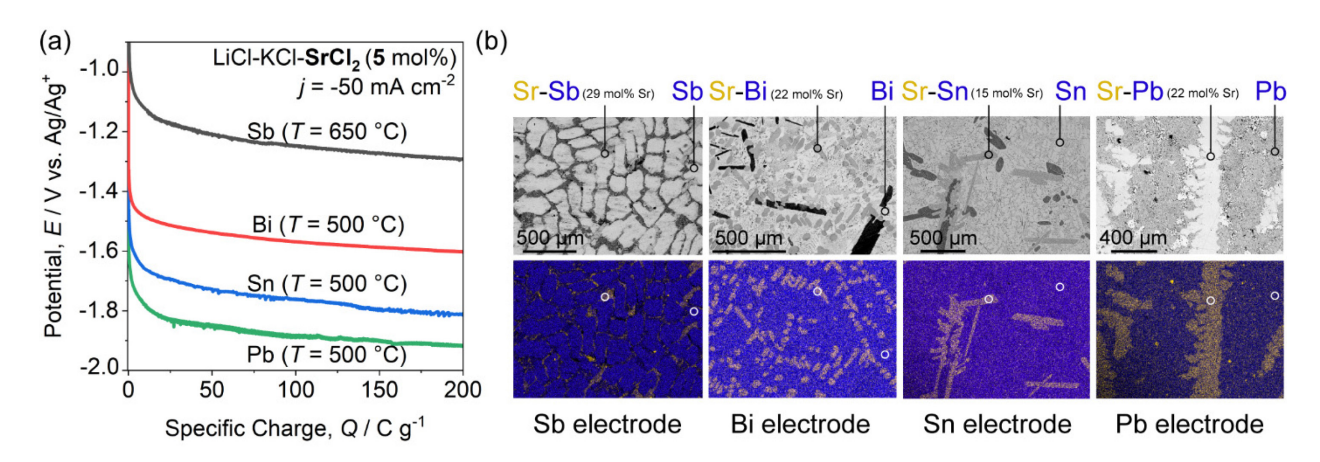


Figure 3: (a) Electrode potential of liquid metal electrodes (Sb, Bi, Sn, Pb) during electrolysis at j = -50 mA cm⁻² in LiCl-KCl-SrCl₂ electrolyte and (b) SEM and elemental X-ray mapping images after electrolysis at 500 °C or 650 °C for Sb (Sr = yellow, liquid metal = dark blue).

Composition of electrolysis products in pure liquid metal electrodes

The composition of electrolysis products (X = Ba, Sr, Li, and K) in the liquid metal electrodes was analyzed using ICP-AES for each electrolyte (Table 1). The mass of each electrolysis product (m_X) was then converted to charge passed (Q_X) using Faraday's law:

$$Q_{\rm X} = \left(\frac{m_{\rm X}nF}{M_{\rm X}}\right) \tag{1}$$

where n is the number of electrons consumed in the reaction (n = 1 for Li and K; n = 2 for Ba and Sr) and M_X is the molar mass. Knowing the total amount of charge passed into the electrode ($Q_{\text{exp}} = 540 \text{ C}$), the Faradaic efficiency was estimated according to:

Faradaic efficiency (%)=
$$\frac{\sum_{X} Q_{X}}{Q_{exp}} \times 100$$
 (2)

Table 1: The composition of electrolysis products in liquid metals at the specific charge of 200 C g⁻¹ in ternary LiCl-KCl-BaCl₂/SrCl₂ electrolytes at 500 °C or 650 °C for Sb by ICP-AES and the estimated Faradaic efficiency.

	Electrolysis products in liquid metal electrodes					
	LiCl-KCl-BaCl ₂ electrolyte					
Liquid metal	Ba (wt%)	Li (wt%)	K (wt%)	Faradaic eff. (%)		
Sb	7.46 (±0.30)	0.36 (±0.01)	0.45 (±0.02)	82.9 (±0.4)		
Bi	8.33 (±0.33)	0.25 (±0.01)	0.31 (±0.01)	79.5 (±0.5)		
Sn	6.14 (±0.25)	0.41 (±0.02)	2.01 (±0.08)	96.1 (±0.3)		
Pb	6.12 (±0.24)	0.46 (±0.02)	0.52 (±0.02)	81.1 (±0.3)		
	LiCl-KCl-SrCl ₂ electrolyte					
	Sr (wt%)	Li (wt%)	K (wt%)	Faradaic eff. (%)		
Sb	3.06 (±0.12)	0.43 (±0.02)	0.16 (±0.01)	65.8 (±0.1)		
Bi	2.53 (±0.10)	0.33 (±0.01)	0.20 (±0.01)	53.2 (±0.1)		
Sn	2.22 (±0.09)	$0.45~(\pm 0.02)$	$0.14~(\pm 0.01)$	57.5 (±0.1)		

Pb $2.04 (\pm 0.08)$ $0.51 (\pm 0.02)$ $0.03 (\pm 0.00)$ $58.1 (\pm 0.1)$

The Faradaic efficiencies from ICP-AES were largely scattered among the electrodes and substantial loss was evident (Table 1). The primary cause for the low and inconsistent Faradaic efficiency is thought to come from sample preparation when deionized water was used to remove entrained salt from the electrode surface, resulting in the loss of reactive alkali and alkaline-earth metals to aqueous solution (e.g., Li + H₂O \rightarrow LiOH(aq) + $\frac{1}{2}$ H₂(g)). Assuming the loss of each electrolysis product is uniform during the sample preparation, the charge for each electrolysis product (Eq. 2) was normalized with respect to $\sum_X Q_X$ in order to estimate the percentage of charge for each electrolysis product (Fig. 4).

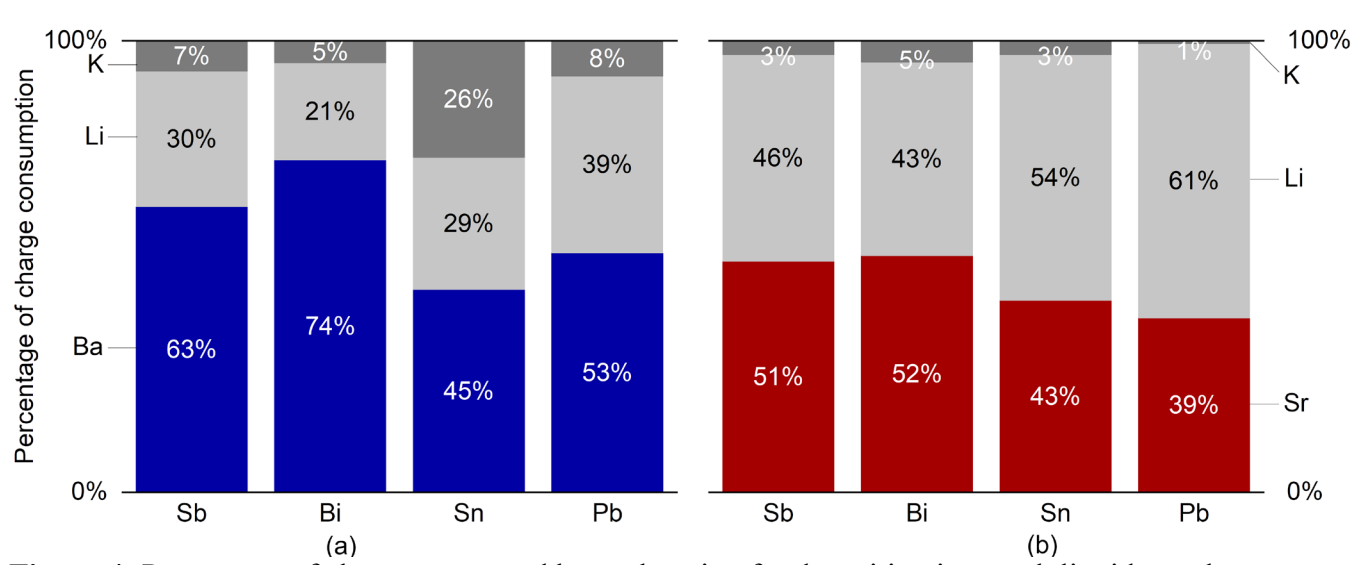


Figure 4: Percentage of charge consumed by each cation for deposition into each liquid metal (Sb, Bi, Sn, Pb) in (a) LiCl-KCl-BaCl₂ and (b) LiCl-KCl-SrCl₂ electrolytes, based on chemical analysis by ICP-AES.

The chemical analysis of electrolysis products confirmed the Ba/Sr recovery by all liquid metal electrodes as well as the co-deposition of Li (Fig. 4). A greater proportion of charge was consumed by Ba²⁺ ions (45-74%) than Sr²⁺ ions (39-52%) during electrolysis from their respective

ternary electrolytes, possibly due to lower activity values of Ba than Sr in the liquid metals. For the liquid Bi and Sb electrodes, a greater percentage of charge was consumed for Ba/Sr deposition than the liquid Sn and Pb electrodes, suggesting their enhanced capability to recover alkaline-earth fission products with less removal of Li and K from molten salts. Despite Ba/Sr having stronger interactions with Sb than Bi, the liquid Bi electrode recovered more Ba and Sr than the Sb electrode. The lower recovery capability of the Sb electrode is thought to come from the higher operating temperature of the Sb electrode (650 °C) that can accelerate side reactions such as the dissolution of Ba and Sr metals into the molten salts.²⁰

Recovery of Ba and Sr into liquid Bi-Sb alloys

The two metals (Bi and Sb) most effective at recovering Ba/Sr were combined as liquid alloy electrodes and investigated to further enhance the recovery of Ba and Sr from the LiCl-KCl electrolyte while minimizing Li/K removal. By forming Bi-Sb alloys (50-50, 60-40, 70-30 mol%), the alloy electrodes take advantage of the strongest interactions of Sb with Ba/Sr (i.e., the largest emf values in Fig. 1) and low melting temperatures for cell operation at 500 °C.²¹ A similar approach was effective in improving the performance of the Li-Sb-Pb liquid metal battery by alloying low-melting Pb with Sb in order to retain the high cell voltage of Sb at 450 °C.²²

Bi-Sb alloy electrodes in LiCl-KCl-BaCl₂: The potential curves of the Bi-Sb alloy electrodes at 500 °C were located between those of liquid Bi and Sb electrodes, and shifted towards that of liquid Bi as Bi content increased (Fig. 5a). After electrolysis, the liquid metal electrodes evolved into a complex microstructure at room temperature (Fig. 5b) with: (i) the preferential segregation of Ba to Sb-rich phases, (ii) a Bi-Sb matrix, and (iii) unidentified regions where Ba, Bi, and Sb are depleted due to the presence of the light-element Li (e.g., dark regions in the Bi-Sb (70-30 mol%) alloy in the SEM image). The preferential segregation of Ba to Sb-rich phases is

thought to originate from the stronger chemical interactions with Sb than Bi, e.g., $a_{\text{Ba(in Sb)}} = 4.4 \times 10^{-17}$ and $a_{\text{Ba(in Bi)}} = 6.8 \times 10^{-16}$ at 500 °C, $x_{\text{Ba}} = 0.05$.^{10,12}

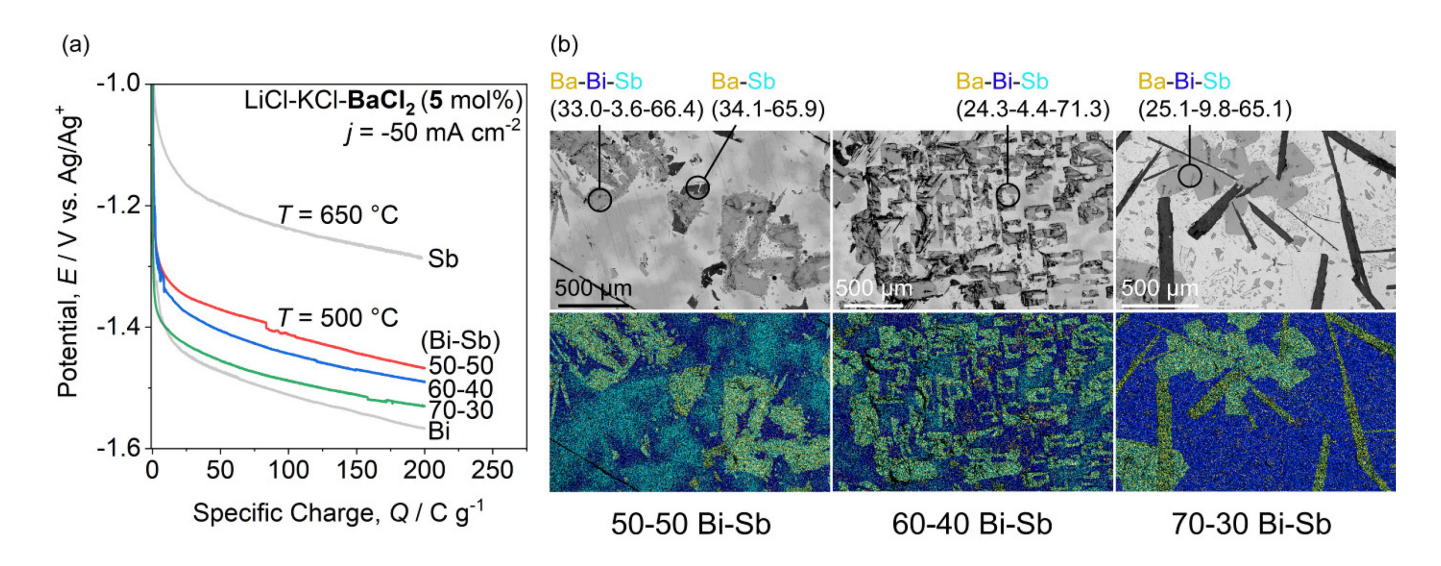


Figure 5: (a) Electrode potential of liquid Bi-Sb alloys (vs. Ag/Ag^+) in LiCl-KCl-BaCl₂ during electrolysis at j = -50 mA cm⁻² and 500 °C, and (b) SEM and elemental X-ray mapping images after electrolysis (Ba = yellow, Bi = dark blue, Sb = light blue).

Table 2: The composition of electrolysis products in liquid Bi-Sb alloys at the specific charge of 200 C g⁻¹ in ternary LiCl-KCl-BaCl₂/SrCl₂ electrolytes at 500 °C by ICP-AES and the estimated Faradaic efficiency.

	LiCl-KCl-BaCl ₂ electrolyte					
Bi-Sb alloys (mol%)						
	Ba (wt%)	Li (wt%)	K (wt%)	Faradaic eff. (%)		
50-50	7.11 (±0.284)	0.12 (±0.005)	0.04 (±0.002)	58.6 (±0.4)		
60-40	6.33 (±0.253)	0.10 (±0.040)	0.07 (±0.003)	52.3 (±0.3)		
70-30	8.95 (±0.358)	0.19 (±0.008)	0.21 (±0.008)	78.8 (±0.6)		
	LiCl-KCl-SrCl ₂ electrolyte					
	Sr (wt%)	Li (wt%)	K (wt%)	Faradaic eff. (%)		

50-50	2.53 (±0.101)	0.44 (±0.018)	0.30 (±0.012)	61.7 (±0.8)
60-40	2.02 (±0.081)	0.49 (±0.020)	0.71 (±0.028)	65.1 (±0.5)
70-30	1.66 (±0.066)	0.68 (±0.027)	1.24 (±0.050)	81.2 (±0.5)

Based on chemical analysis by ICP-AES (Table 2), the percentage of charge for each electrolysis product was estimated (Fig. 6). As Sb content increased, the percentage of charge increased up to 85% for Ba deposition and decreased down to 13-14% for Li deposition, suggesting enhanced recovery capability of Bi-Sb alloys compared to pure Bi and Sb. Based upon the increased Ba deposition into Bi-Sb alloys and the preferential segregation of Ba to the Sb-rich phases, it is reasonable to suggest that alloying Sb enhances Ba recovery by utilizing the strong chemical interactions between Ba and Sb at 500 °C.

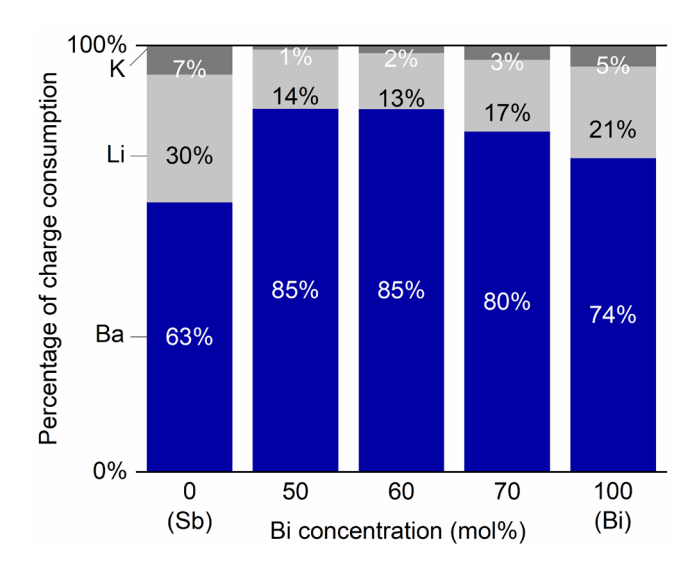


Figure 6: Percentage of charge consumed by each electrolysis product in liquid Bi-Sb alloys (50-50, 60-40, 70-30 mol%) at 500 °C in LiCl-KCl-BaCl₂, compared to liquid Bi and Sb (650 °C).

<u>Bi-Sb alloy electrodes in LiCl-KCl-SrCl₂</u>: During the initial stage of electrolysis using the Bi-Sb alloy electrodes in LiCl-KCl-SrCl₂, the potential curves lie between those of pure Bi and Sb (Fig. 7a), similar to the behavior observed in the LiCl-KCl-BaCl₂ electrolyte. The Bi-Sb (50-50)

mol%) alloy exhibited a smooth potential curve up to 200 C g⁻¹; however, the other Bi-Sb alloys (60-40 and 70-30 mol%) exhibited a steep potential drop during electrolysis, indicating a significant overpotential possibly due to the formation of a solid phase (nucleation overpotential) and transition into a complex phase behavior. After electrolysis, the compositions of electrolysis products in the Bi-Sb alloy electrodes were analyzed by ICP-AES (Table 2).

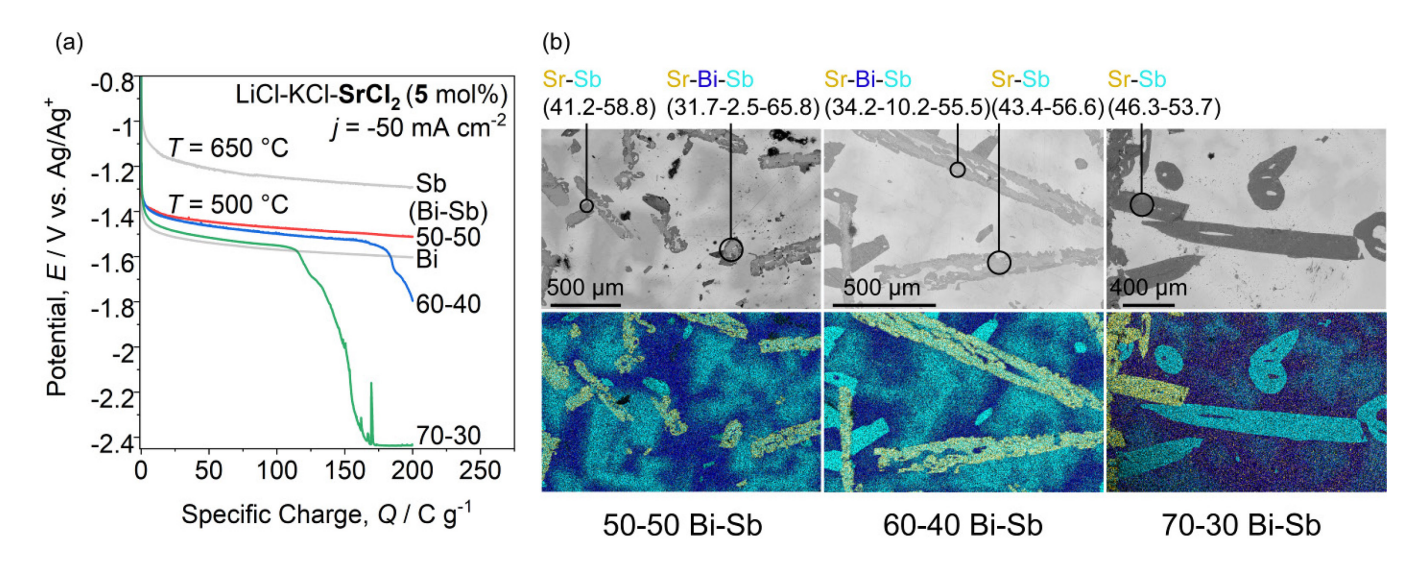


Figure 7: (a) Electrode potential of liquid Bi-Sb alloys (vs. Ag/Ag^+) in LiCl-KCl-SrCl₂ during constant-current electrolysis at j = -50 mA cm⁻² and 500 °C, and (b) SEM and elemental X-ray mapping images after electrolysis (Sr = yellow, Bi = dark blue, Sb = light blue).

The microstructure of Bi-Sb alloys at room temperature confirmed a preferential segregation of Sr to Sb-rich phases (Fig. 7b). A distinct Sr-deficient phase was clearly observed in the Bi-Sb (60-40 and 70-30 mol%) electrodes, indicating the co-deposition of Li. According to the percentage of charge for each electrolysis product (Fig. 8), these two Bi-Sb alloys contained a greater proportion of charge for Li deposition (52-59%) and increased level of K (14-19%), both of which could be attributed to the large overpotential. Although the increased Sb content in Bi-Sb alloys enhanced Sr recovery up to 45% and decreased Li deposition down to 49%, the Sr

recovery capability of the liquid Bi-Sb alloys was poor compared to the pure Bi and Sb electrodes, based upon the deposition of less Sr and more Li from the LiCl-KCl-SrCl₂ salt.

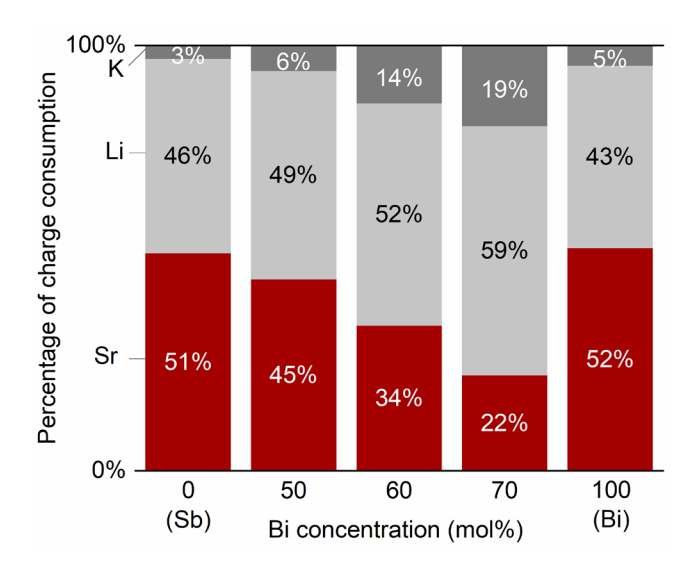


Figure 8: Percentage of charge consumed by each electrolysis product in liquid Bi-Sb alloys (50-50, 60-40, 70-30 mol%) at 500 °C in LiCl-KCl-SrCl₂, compared to liquid Bi and Sb (650 °C).

Overall, the alloying of Sb with Bi improved the recovery capability for Ba recovery; however, it was not effective for Sr recovery possibly due to a complex phase behavior of the multi-component alloy electrode (e.g. Bi-Sb-Sr-Li) during electrolysis.

CONCLUSION

Alkaline-earth metals Ba and Sr were successfully recovered from the LiCl-KCl eutectic electrolyte by electrochemical deposition into liquid metal electrodes by leveraging the strong atomic interactions between alkaline-earth metals and liquid metals. Of the pure liquid metal electrodes investigated, liquid Bi and Sb exhibited greater Ba/Sr recovery than liquid Sn and Pb based upon electrolysis products by ICP-AES. The liquid Bi-Sb alloy electrodes at 500 °C achieved enhanced Ba recovery compared to pure Bi and Sb (650 °C), and the greater the proportion of Sb in the electrode, the greater the Ba recovery. However, the Bi-Sb electrodes were less effective for Sr recovery than either the Bi or Sb electrodes. During electrochemical

deposition, Li and K were co-deposited into the pure liquid metals and liquid Bi-Sb alloys; possibly leading to complex phase behavior that influenced Ba/Sr recovery. These comprehensive results indicate that liquid metals and alloys can be used to recover alkaline-earth fission products that accumulate in molten salts during used nuclear fuel recycling processes and minimize additional nuclear waste generated during the recycling process.

AUTHORSHIP DETAILS

Present Address:

^a Chemical and Fuel Cycle Technologies, Argonne National Laboratory 9700 S. Cass Avenue, Lemont, IL 60439, USA.

ACKNOWLEDGEMENTS

This work was supported by the US National Science Foundation (grant number: CMMI-1662817) and the US Department of Energy, Office of Nuclear Energy's Nuclear Engineering University Program (Award No. DE-NE0008757).

REFERENCES

- (1) Electrometallurgical Techniques for DOE Spent Fuel Treatment: Final Report; National Research Council, National Academies Press: Washington, DC, 2000; 1-116, DOI: 10.17226/9883.
- (2) Williamson, M. A.; Willit, J. L. Pyroprocessing Flowsheets for Recycling Used Nuclear Fuel. *Nucl. Eng. Technol.* **2011**, *43* (4), 329–334, DOI: 10.5516/NET.2011.43.4.329.
- (3) Bruno, J., Ewing, R. C. Spent Nuclear Fuel. *Elements* **2006**, *2*, 343–349, DOI: 10.2113/gselements.2.6.343.
- (4) Gutknecht, T. Y.; Fredrickson, G. L.; Utgikar, V. *Thermal Analysis of Surrogate*Simulated Molten Salts with Metal Chloride Impurities for Electrorefining Used Nuclear

 Fuel; INL/EXT-11-23511; 2012; 1-144, DOI: 10.2172/1055967.

- (5) Commercial Nuclear Waste: Resuming Licensing of the Yucca Mountain Repository

 Would Require Rebuilding Capacity at DOE and NRC, Among Other Key Steps; GAO-17
 340; U.S. Government Accountability Office: Washington, DC, April 2017; 1-48.
- (6) Bale, C. W.; Bélisle, E.; Chartrand, P.; Decterov, S. A.; Eriksson, G.; Gheribi, A. E.; Hack, K.; Jung, I. H.; Kang, Y. B.; Melançon, J.; Pelton, A. D.; Petersen, S.; Robelin, C.; Sangster, J.; Spencer, P.; Van Ende, M. A. FactSage Thermochemical Software and Databases, 2010–2016. *Calphad.* 2016, 54, 35–53, DOI: 10.1016/j.calphad.2016.07.004.
- (7) Matsumiya, M.; Takano, M.; Takagi, R.; Fujita, R. Recovery of Ba²⁺ Using Liquid Metallic Cathodes in Molten Chlorides. *J. Nucl. Sci. Technol.* **1998,** *35* (11), 836–839, DOI: 10.3327/jnst.35.836.
- (8) Matsumiya, M.; Takagi, R.; Fujita, R. Recovery of Eu²⁺ and Sr²⁺ Using Liquid and KCl Metallic System Cathodes in Molten NaCl-KCl and KCl System. *J. Nucl. Sci. Technol.* 1997, 34 (3), 310–317, DOI: 10.3327/jnst.34.310.
- (9) Lichtenstein, T.; Nigl, T. P.; Smith, N. D.; Kim, H. Electrochemical Deposition of Alkaline-Earth Elements (Sr and Ba) from LiCl-KCl-SrCl₂-BaCl₂ Solution Using a Liquid Bismuth Electrode. *Electrochim. Acta* 2018, 281, 810–815, DOI: 10.1016/j.electacta.2018.05.097.
- (10) Lichtenstein, T.; Smith, N. D.; Gesualdi, J.; Kumar, K.; Kim, H. Thermodynamic Properties of Barium-Bismuth Alloys Determined by Emf Measurements. *Electrochim*. *Acta* 2017, 228, 628–635, DOI: 10.1016/j.electacta.2017.07.113.
- (11) Smith, N.; Lichtenstein, T.; Gesualdi, J.; Kumar, K.; Kim, H. Thermodynamic Properties of Strontium-Bismuth Alloys Determined by Electromotive Force Measurements.

 Electrochim. Acta 2016, 225, 584–591, DOI: 10.1016/j.electacta.2016.12.051.

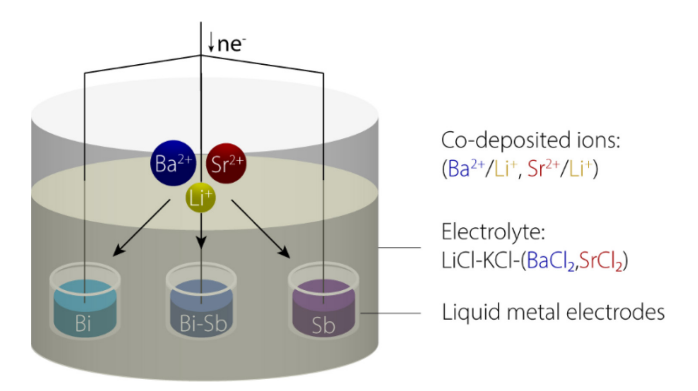
- (12) Lichtenstein, T.; Gesualdi, J.; Nigl, T. P.; Yu, C. T.; Kim, H. Thermodynamic Properties of Barium-Antimony Alloys Determined by Emf Measurements. *Electrochim. Acta* **2017**, 251, 203–211, DOI: 10.1016/j.electacta.2017.07.113.
- (13) Smith, N. D.; Orabona, N.; Lichtenstein, T.; Gesualdi, J.; Nigl, T. P.; Kim, H.

 Thermodynamic Properties of Sr-Sb Alloys via Emf Measurements Using Solid CaF₂-SrF₂

 Electrolyte. *Electrochim. Acta* **2019**, *305*, 547–554, DOI: 10.1016/j.electacta.2019.02.124.
- (14) Lichtenstein, T.; Gesualdi, J.; Yu, C. T.; Kim, H. Thermochemical Properties and Phase Transitions of Ba–Sn Alloys from Thermal Characterization and Emf Measurements. *J. Alloys Compd.* **2019**, *811*, 151531, DOI: 10.1016/j.jallcom.2019.07.243.
- (15) Smith, N. D.; Paz Soldan-Palma, J.; Kong, Y.; Liu, Z.-K.; Kim, H. Thermodynamic Properties of Sr–Sn Alloys via Emf Measurements and Thermal Analysis. *J. Electrochem. Soc.* **2020**, *167*, 082508, DOI: 10.1149/1945-7111/ab8de1.
- (16) Gesualdi, J.; Nigl, T. P.; Lichtenstein, T.; Smith, N. D.; Kim, H. Thermodynamic Properties of Ba-Pb Alloys Determined by Emf Measurements Using Binary CaF₂-BaF₂ Electrolyte. *J. Electrochem. Soc.* **2019**, *166* (8), D268–D275, DOI: 10.1149/2.0191908jes.
- (17) Nigl, T. P.; Lichtenstein, T.; Smith, N. D.; Gesualdi, J.; Kong, Y.; Kim, H.
 Thermodynamic Properties of Strontium-Lead Alloys Determined by Electromotive Force
 Measurements. J. Electrochem. Soc. 2018, 165 (14), H991–H998, DOI:
 10.1149/2.1091814jes.
- (18) Ojwang, D. O.; Bobev, S. Synthesis and Structural Characterization of Ba₇Li₁₁Bi₁₀ and AE₄(Li,Tr)₇Pn₆ (AE = Sr, Ba, Eu; Tr = Ga, In; Pn = Sb, Bi). *Inorganics* **2018**, *6* (4), 109, DOI: 10.3390/inorganics6040109.
- (19) Lichtenstein, T.; Nigl, T. P.; Kim, H. Recovery of Alkaline-Earths into Liquid Bi in

- Ternary LiCl-KCl-SrCl₂/BaCl₂ Electrolytes at 500 °C. *J. Electrochem. Soc.* **2020**, *167*, 102501, DOI: 10.1149/1945-7111/ab9758.
- (20) Dworkin, A. S.; Bronstein, H. R.; Bredig, M. A. Miscibility of Liquid Metals with Salts.
 VIII. Strontium-Strontium Halide and Barium-Barium Halide Systems. *J. Phys. Chem.* 1968, 72 (6), 1892–1896, DOI: 10.1021/j100852a006.
- (21) Feutelais, Y.; Morgant, G.; Didry, J. R. Thermodynamic Evaluation of the System Bismuth-Antimony. *Calphad* **1992**, *16* (2), 111–119, DOI: 10.1016/0364-5916(92)90001-E.
- (22) Wang, K.; Jiang, K.; Chung, B.; Ouchi, T.; Burke, P. J.; Boysen, D. A.; Bradwell, D. J.; Kim, H.; Muecke, U.; Sadoway, D. R. Lithium-Antimony-Lead Liquid Metal Battery for Grid-Level Energy Storage. *Nature* 2014, 514 (7522), 348–350, DOI: 10.1038/nature13700.

For Table of Contents Use Only:



Synopsis:

Electrochemical co-deposition of Ba^{2+}/Sr^{2+} and Li^+ into liquid metal electrodes in molten chlorides to remove fission products from molten salts and close the nuclear fuel cycle.